Adsorption of Reactive Dyes from Wastewater Using Cationic Surfactant-modified Coffee Husk Biochar

Chatsuda Kosaiyakanon and Suratsawadee Kungsanant*

Department of Chemical Engineering, Faculty of Engineering, Prince of Songkla University, Hat-Yai, Songkhla 90110, Thailand

ARTICLE INFO

Received: 28 Feb 2019
Received in revised: 4 Jun 2019
Accepted: 14 Jun 2019
Published online: 30 Jul 2019
DOI: 10.32526/ennrj.18.1.2020.03

Keywords:
Reactive dye/ Coffee husk/ Biochar/ Cationic surfactant/ Dye adsorption

*** Corresponding author:**
E-mail: suratsawadee.k@psu.ac.th

ABSTRACT

A solid agricultural waste, coffee husk, was applied as an adsorbent for reactive dye-polluted wastewater treatment. Coffee husk biochar was pyrolyzed at 450 °C and then chemically activated using 50% $ZnCl_2$ solution. The surface of activated coffee husk biochar was modified using a cationic surfactant, Cetyltrimethylammonium bromide (CTAB), to create CTAB-modified coffee husk biochar (MCH), to improve reactive adsorption of anionic dyes from synthetic wastewater. The selected reactive dyes were reactive yellow 145 (RDY145), reactive red 195 (RDR195), and reactive blue 222 (RDB222). The adsorption kinetics fit well using a pseudo-second order model for all three dyes. The adsorption isotherms matched well with the Langmuir model . The removal efficiency of RDY145 (83.7%) was the highest, followed by RDR195 (71.1%) and RDB222 (59.6%). The amount of RDY145 adsorbed by MCH was about 9-fold that adsorbed by conventional activated carbon. Additionally, the solution pH had no effect on reactive dye removal efficiency using MCH.

1. INTRODUCTION

The growth of textile industry plays an important economic role in Thailand but its large water consumption creates a considerable amount of wastewater effluents. Dyes released to the environment are estimated at around 200,000 tons annually (Ogugbue and Sawidis, 2011). Normally, the dyes in textile industry are categorized as anionic (acid, direct, and reactive dyes), cationic (basic dyes), and nonionic dyes (dispersed dyes) (Ghazi Mokri et al., 2015). Generally, around 20 to 30% of the dyes used are of a reactive type, so representatives of these were selected for this study. Reactive dyes are also known as azo dyes because they contain one or more azo groups (-N=N-). In addition, reactive dyes containing aromatic amines can decompose and the amine groups formed are suspected to be carcinogenic (Mook et al., 2016; Moazzam et al., 2017). Thus, improper wastewater treatment can have negative environmental impacts affecting aquatic life and ecosystems.

Reactive dye contaminants should be removed from wastewaters. There are several methods to remove dyes from industrial effluents, including adsorption by activated carbon, electrochemical or membrane separations, and coagulation (Sun et al., 2013; Mook et al., 2016; Puasa et al., 2018). Among these, adsorption by activated carbon (AC) is a well-known technique for dye removal. The advantages of this technique include comparatively small need of land area, environmental friendliness, and ease of operation. However, the cost of AC remains the key to economic feasibility.

Nowadays, agricultural residues with high carbon content, such as palm shell, coconut coir, and rice husk have been studied as potential alternative adsorbents for AC (Sun et al., 2013; Ahmad et al., 2014; Mook et al., 2016; Mi et al., 2016). Typically, they can be applied to produce biochar by thermal degradation in oxygen-limited conditions, and consequently utilized as a low-cost adsorbent for pollutant separation from air, or heavy metals as well as textile dye removal from wastewater (Mi et al., 2016; Moazzam et al., 2017; Rehman and Razzaq, 2017). Biochar adsorption has been intensively studied because it has excellent adsorption capability and satisfies the need for cost effective adsorbents.

In southern Thailand, Robusta coffee has been planted on a large scale and it accounts for 98% of the coffee production in Thailand (Maleangpoothong

Citation: Kosaiyakanon C, Kungsanant S. Adsorption of reactive dyes from wastewater using cationic surfactant-modified coffee husk biochar. Environ. Nat. Resour. J. 2020;18(1):21-32. DOI: 10.32526/ennrj.18.1.2020.03

et al., 2013). Consequently, abundant amounts of coffee husk are generated and these could be converted to AC, as the husks are highly porous with high carbon content. Additionally, making biochar from coffee husk is not only promising for agricultural waste minimization, but it provides value-added adsorbents.

Furthermore, many studies have reported that adsorption with biochar is effective in the removal of reactive dyes from aqueous solution, such as reactive black 5 removal using palm shell biochar (Mook et al., 2016), reactive red 2 removal using coir pith biochar (Thitame and Shukla, 2016), and reactive blue 171 removal using *Enteromorpha prolifera* biochar (Sun et al., 2013). Besides, surface modification of the biochar with surfactants could enhance the adsorption capacity and ensure environmental friendliness (Puasa et al., 2018). Mi et al. (2016) reported that biochar prepared from cornstalk and modified by Cetyltrimethylammonium bromide (CTAB) had up to 53% improved adsorption of negatively charged anionic dye from water. In addition, all the studies have agreed that using biochar as a precursor for AC for reactive dye removal provided a great adsorption performance, cheap treatment costs, no unexpected by-products, and minimal waste. Thus, biochar was suggested to be promising for AC development.

Therefore, this work aimed to apply the CTAB-modified coffee husk biochar (MCH) for reactive dye removal from synthetic wastewater. The reactive dyes were reactive yellow 145 (RDY145), reactive red 195 (RDR195) , and reactive blue 222 (RDB222). The dye removal and adsorption capacities of MCH and AC are compared and discussed in terms of kinetic models and adsorption isotherms. The effects of pH on reactive dye removal using MCH are also discussed.

2. METHODOLOGY

2.1 Materials

Husk of Robusta coffee was obtained from Thamsing Coffee Group Community Enterprise, located in Tham Sing sub-district, Mueang Chumphon district, Chumphon province, Thailand. The geographic location of coffee plantation is at latitude from 10°22'45.19"N to 10°26'28.82"N and longitude from 99°02'13.11"E to 99°07'19.75"E. The plantation covers an area of 2,891 ha, as shown in Figure 1 (GEO-Informatics Research Center for Natural Resource and Environment, Southern Regional Center of Geo-Informatics and Space Technology, 2019). The coffee husk was dried under sunlight for 4 days. It was then pyrolyzed at 450 °C for 1.5 h in a furnace tube under nitrogen atmosphere to remove the volatile matter (Ahmad et al., 2014). The obtained coffee husk biochar (CH) was then crushed and controlled for size in the range 0.6-1.41 mm. Food grade AC made from coconut shell was purchased from C. Gigantic Carbon Co., Ltd., Thailand. The cationic surfactant (CTAB) and zinc chloride ($ZnCl_2$) were purchased from Ajax Finechem Pty Ltd. (100% purity). All commercial reactive dyes (RDY145, RDR195, and RDB222) were received from KPT Corporation (Thailand) Co., Ltd. , Thailand. The properties of chemicals are summarized in Table 1. All the chemicals were used as received.

2.2 CH activation

A quantity of 50 g of CH was impregnated with 150 g of 50%wt. $ZnCl_2$ solution and left at room temperature for 24 h. Then, it was dried in an oven at 105 °C for 24 h, followed by heating at 500 °C for 2 h in a furnace tube under nitrogen blanket at a flow rate of 0.25 L/min (Mozammel et al., 2002; Kula et al., 2008). The obtained activated coffee husk biochar (ACH) sample was washed with distilled water until the pH of water was neutral. Then, it was dried again in the oven at 105 °C for 24 h.

2.3 ACH pretreatment using cationic surfactant

A quantity of 10 g of ACH was mixed with 1,000 mL of 7.5 mM CTAB solution. The samples were shaken for 7.5 h in the incubator shaker at 30 °C and 170 rpm shaking speed. After that, the obtained MCH samples were washed and dried at 60 °C for 15 h, and finally stored in desiccators for further use (Lin et al., 2013).

2.4 Adsorption study

A 1 g quantity of MCH was mixed with 100 mL of synthetic wastewater containing a reactive dye (RDY145, RDR195, or RDB222). The concentrations of reactive dyes were varied in the range 50-700 mg/L. The sample bottles were kept in an incubator shaker at 30 °C with 170 rpm shaking speed. Liquid samples were collected from each bottle every 10 min and were immediately analyzed for residual dye concentration using a UV-Visible Spectrophotometer (HP 8453) at 417, 541, and 614 nm for RDY145, RDR195, or RDB222, respectively.

The pH of the solutions was adjusted by adding HCl or NaOH solution (1 mol/L) (Oei et al., 2009; Ghazi Mokri et al., 2015). The cases were run randomly in triplicate and the standard deviation was less than 4%. The standard deviation is shown as y-error bars in graphs of Figures 3, 4, 5, and 7.

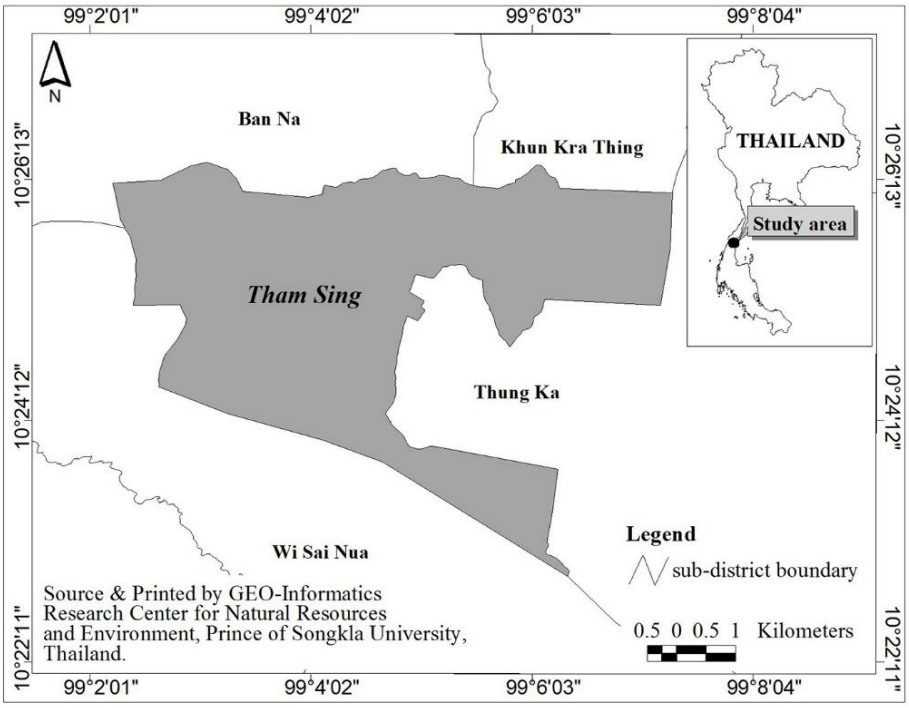

Figure 1. Map of coffee plantation, Tham Sing sub-district in Mueang Chumphon District, Chumphon Province, Thailand (GEO-Informatics Research Center for Natural Resource and Environment, Southern Regional Center of Geo-Informatics and Space Technology, 2019).

Table 1. The chemicals used in this study

Chemical	Scientific name	Molecular formula	Molecular weight (MW, g/mol)
CTAB[a]	Cetyltrimethylammonium bromide	$C_{19}H_{42}BrN$	364.5
RDY145[b]	Tetrasodium;7-[[2-(carbamoylamino)-4-[[4-chloro-6-[3-(2-sulfonatooxyethyl sulfonyl)anilino]-1,3,5-triazin-2-yl] amino]phenyl]diazenyl]naphthalene-1,3,6-trisulfonate	$C_{28}H_{20}ClN_9Na_4O_{16}S_5$	1026.2
RDR195[c]	Pentasodium;(3E)-5-[[4-chloro-6-[3-(2-sulfonatooxyethylsulfonyl)anilino]-1,3,5-triazin-2-yl]amino]-3-[(1,5-disulfonatonaphthalen-2-yl)hydrazinylidene]-4-oxonaphthalene-2,7-disulfonate	$C_{31}H_{19}ClN_7Na_5O_{19}S_6$	1136.3
RDB222[d]	Hexasodium;5-amino-3-[(1,5-disulfonatonaphthalen-2-yl)diazenyl]-4-oxido-6-[[3-sulfonato-5-[[4-[4-(2-sulfooxyethyl sulfonyl)anilino]-1,3,5-triazin-2-yl] amino]phenyl]diazenyl]naphthalene-2,7-disulfonate	$C_{37}H_{24}N_{10}Na_6O_{22}S_7$	1323.0

Remark: Letters a, b, c, and d express data cited from NCBI (2004), NCBI (2005), Guidechem (2017), and NCBI (2015), respectively.

2.5 Data analysis

For the kinetics study, the quantity of adsorbed dyes per unit weight of adsorbent was calculated as in Equation (1), and the dye removal efficiency (% Sorption) was determined with Equation (2) (Amin, 2008; de Franco et al., 2017):

$$q_t = \frac{C_0 - C_t}{m} V \quad (1)$$

$$\% \text{ Sorption} = \frac{C_0 - C_t}{C_0} \times 100 \quad (2)$$

Here, C_0 is the initial dye concentration (mg/L), C_t is the residual dye concentration in the solution after adsorption, V is the solution volume (L), and m is the mass of adsorbent (g) (Mi et al., 2016).

Then, the adsorption kinetics was assessed against both pseudo-first order and pseudo-second order models. The pseudo first order model is based on assumed physical multilayer absorption that is reversible.In contrast, the pseudo-second order model assumes chemical monolayer adsorption that is irreversible (Ibrahim et al., 2010; Ghazi Mokri et al., 2015; Mook et al., 2016). The pseudo-first order and pseudo-second order equations are presented as Equation (3) and Equation (4), respectively:

$$\ln\left(\frac{q_e}{q_e - q_t}\right) = k_1 t \quad (3)$$

$$q_t = \frac{q_e^2 k_2 t}{1 + q_e k_2 t} \quad (4)$$

Here, q_t is the amount of adsorbed dye on adsorbent (mg/g), q_e is amount of adsorbed dye on adsorbent at equilibrium (mg/g), k_1 is the rate constant of pseudo-first order model (min^{-1}), k_2 is the rate constant of pseudo-second order model (g/mg-min), and t is the time (min) (Ibrahim et al., 2010; Ghazi Mokri et al., 2015; Mook et al., 2016; de Franco et al., 2017).

Equilibrium dye adsorption isotherms were plotted as suggested by Langmuir and Freundlich models. The Langmuir model describes monolayer adsorption on a homogenous surface. The Freundlich model describes multilayer adsorption on a heterogeneous surface (Ibrahim et al., 2010; Ghazi Mokri et al., 2015; Mi et al., 2016). The Langmuir and Freundlich models are expressed in Equation (5) and Equation (6), respectively:

$$\frac{q_e}{q_{max}} = \frac{k_L C_e}{1 + k_L C_e} \quad (5)$$

$$q_e = k_f C_e^{1/n} \quad (6)$$

Here, q_e is the amount of adsorbed dye on the adsorbent at equilibrium (mg/g), q_{max} is the maximum adsorption of dye on the adsorbent (mg/g), C_e is residual dye concentration at equilibrium (mg/L), k_L is Langmuir constant related to the energy of adsorption (L/mg), k_F is Freundlich constant indicating adsorption capacity (mg/g $(L/mg)^{1/n}$), and n is Freundlich exponent accounting for adsorption intensity or the energetic heterogeneity of the adsorbing surface (de Franco et al., 2017; Markandeya et al., 2017). Additionally, the dimensionless separation factor (R_L) from the Langmuir model could indicate the affinity of adsorbent to adsorbate and is determined using Equation (7):

$$R_L = \frac{1}{1 + k_L C_0} \quad (7)$$

Here, a value of R_L equal to zero indicates that the adsorption is irreversible, while R_L in the range from zero to one indicates favorable adsorption. Besides, if R_L is equal to one, then adsorption is linear. A value of R_L greater than one represents unfavorable adsorption (Meng et al., 2018; Wang et al., 2018).

3. RESULTS AND DISCUSSION

3.1 Characterization of adsorbents

The surfaces of studied adsorbents, designated as CH, ACH, MCH, and AC, were imaged using SEM, as shown in Figure 2.

It can be seen that the pores of the ACH and MCH were similar and larger than those observed in CH and AC. The use of $ZnCl_2$ solution in activation could create more pores onto the CH surfaces resulting in increasing the porosity of CH. SEM images also indicate that the adsorption of CTAB on adsorbent MCH surfaces (Figure 2(c)) provides surface structure similar to ACH (Figure 2(b)). The pores of ACH and MCH are large and randomly distributed on the surfaces, whereas, the pores of AC are quite small and uniform. In addition, the porosities and surface areas of all adsorbents were assessed using the BET technique, with results listed in Table 2.

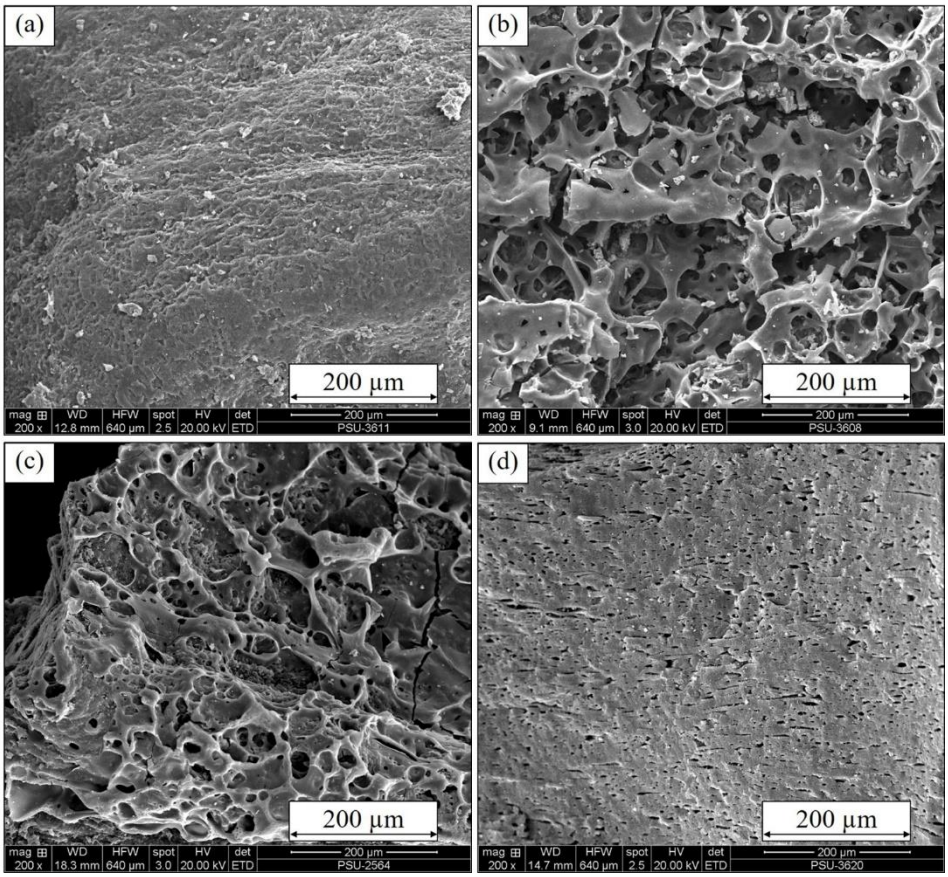

Figure 2. SEM images of CH (a), ACH (b), MCH (c), and AC (d) at × 200

Table 2. BET surface area analysis for the adsorbents

Parameter	CH	ACH	MCH	AC
BET surface area (m^2/g)	0.5	750.1	557.4	1099.8
Adsorption average pore diameter (Å)	43.4	18.9	22.9	17.0
Pore volume (cm^3/g)	0.0006	0.3541	0.3192	0.4684

The results from BET analysis agree well with the SEM images. It could be noted that the surface area and pore volume of ACH were significantly higher than those of CH, due to activation, while its average pore diameter was decreased. The increase in porosity was caused by removal of ash, tar, and nonvolatile residues from CH surfaces in the $ZnCl_2$ solution. However, as the ACH was modified using CTAB to obtain the MCH, the pores of MCH are wider and its surface area is slightly lower than those of ACH. This might be caused by further removal of organic residues in CTAB from ACH surfaces increasing the pore diameter and reducing the surface area of MCH.

According to the pore size diameter, MCH could be classified as mesoporous material with pore diameters in the range 20-500 Å, whereas the AC having pore diameters less than 20 Å is considered microporous (Ip et al., 2009). Though surface area and pore volume of MCH are lower and pore diameter is slightly larger than for the AC, many studies have reported that the specific surface area of synthesized biochar for reactive dye removal from wastewater should be in the range 600-900 m^2/g (Vijayaraghavan et al., 2009; Sun et al., 2013; Mook et al., 2016; Thitame and Shukla, 2016). In this study, the specific surface area of MCH was slightly lower than those in prior reports. Therefore, the use of MCH as an AC alternative for reactive dye removal is challenging and should be intensively examined.

3.2 Comparative adsorption of the reactive dyes by ACH, MCH, and AC

The sorbent dosage was fixed at 1 g. The adsorbents, namely ACH, MCH, and AC, were used for RDY145 removal from synthetic wastewater. The

initial RDY145 concentration was 700 mg/L. The experiment was conducted at pH 7, 30 °C, and 170 rpm shaking speed for 3 h. The RDY145 removal efficiencies by ACH, MCH, and AC are shown in Figure 3.

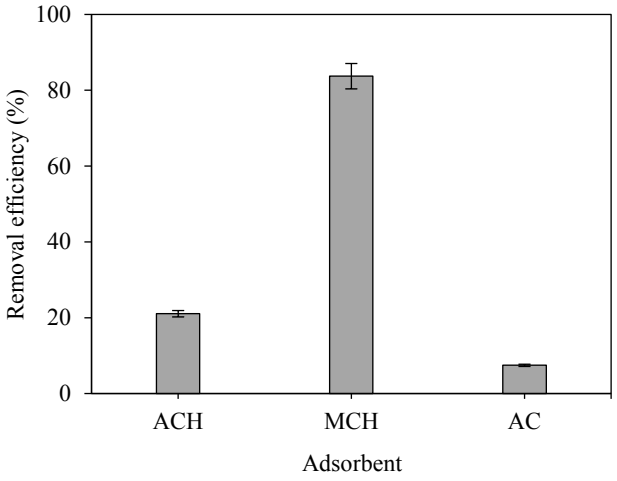

Figure 3. RDY145 removal efficiencies by ACH, MCH, and AC. Operating conditions: 700 mg/L of C_0, 30 °C, pH 7, and 170 rpm shaking speed for 3 h.

The results show 20, 83, and 7% removal of RDY145 by ACH, MCH, and AC, respectively. Interestingly, the higher adsorption efficiency of ACH than that of AC indicates that wider pores could facilitate reactive dye molecule accessibility to interior pore surfaces resulting in better reactive dye adsorption. This result combined with the data in Table 2 demonstrates that pore size of an adsorbent plays a crucial role in reactive dye removal. In addition, the MCH could increase RDY145 removal efficiency by up to 4-fold of ACH and 11-fold of AC, respectively. The increase in adsorption affinity for anionic dye might be due to CTAB modifying the surface charges on ACH. Our preliminary study shows that the ACH had a large capacity to adsorb CTAB (around 78.6% of the initial CTAB dosage) because of the large specific surface and hydrophobic attraction. CTAB could be adsorbed as individual molecules on the ACH surface, forming a monolayer, following the Langmuir adsorption isotherm (data not shown). The cationic surfactant CTAB has both a polar hydrophilic head (positive charge) and a non-polar hydrophobic tail. The tails of CTAB adsorb on hydrophobic sites of the ACH surface through Van der Waals attraction forces (Krivova et al., 2013; Ahmad et al., 2014; Puasa et al., 2018). Additionally, the positively charged heads can effectively adsorb negatively charged RDY145 molecules from wastewater by electrostatic interactions (Mi et al., 2016; Puasa et al., 2018). Thus, the MCH modified with this cationic surfactant has potential for anionic dye removal from wastewater.

3.3 Effect of pH on RDY145 removal using MCH

The removal of RDY145 from wastewater using MCH was tested at 700 mg/L C_0, 1 g of MCH, 30 °C, and 170 rpm shaking speed. The pH of wastewater from textile industry in Thailand is reported to be in the range 7-9 (Department of Industrial Works, Ministry of Industry, 2013). Typically, dye adsorption is a pH dependent process. The variation of pH in bulk solution could impact the surface properties of adsorbent and disturb the adsorbent-adsorbate interaction. Thus, in this work, the pH of solution was set at 3, 6, or 9 using HCl or NaOH. The relationship between adsorption and pH of solution is shown in Figure 4.

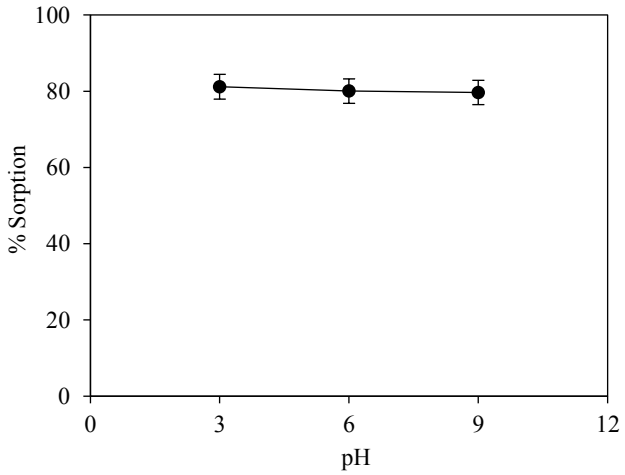

Figure 4. The adsorption percentages of RDY145 at different pH. Operating conditions: 700 mg/L of C_0, 1 g of MCH, 30 °C, and 170 rpm shaking speed.

It is seen that the pH of the solution had no effect on RDY145 removal efficiency. When NaOH was added to increase the pH, the small extra amount of hydroxyl groups (OH^-) present in the solution did not significantly interfere with adsorption of RDY145 on binding sites of MCH. Similarly, HCl decreased solution pH and provided free hydrogen ions (H^+), but these did not alter the positively charged CTAB-modified surface of MCH. Therefore, the removal efficiency of RDY145 was unaffected. These results were also consistent with the studies of pH variation in the range of 3-9 on reactive dyes removal using AC. They reported that the variation of solution pH had no effect on reactive dyes' removal

efficiency (Nabil et al., 2014; Mook et al., 2016). Thus, the observed results also support the use of MCH as an alternative for AC application in a variety of environmental pH.

3.4 Adsorption of reactive dyes

A 1 g quantity of MCH was applied for reactive dyes (RDY145, RDR195, or RDB222) removal from synthetic wastewater, indicated by MCH-RDY145, MCH-RDR195, or MCH-RDB222 as shown in Figure 5. Besides, the dye removal efficiencies of MCH and AC were compared using RDY145, with these cases labeled as MCH-RDY145 and AC-RDY145 in Figure 5, respectively. The quantity of AC was also controlled at 1 g. The particle sizes of the adsorbents were similar and controlled within 0.6-1.41 mm. The initial dye concentration was 700 mg/L. The experiment was conducted at pH 7, 30 °C, and 170 rpm shaking speed. The relationship between the adsorbed reactive dye quantity and contact time is shown in Figure 5.

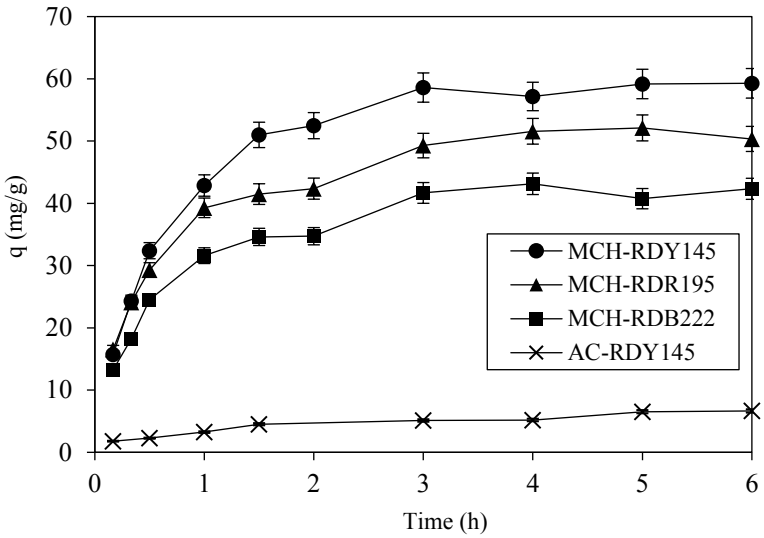

Figure 5. Reactive dye adsorption at various contact times for MCH-RDY145, MCH-RDR195, MCH-RDB222, and AC-RDY145, respectively. Operating conditions: 700 mg/L of C_0, 30 °C, pH 7, and 170 rpm shaking speed.

The results show that dye adsorption rapidly increased with contact time at initial uptake, after which it slowly increased and eventually saturated. The adsorption process reached equilibrium within 3 h for all reactive dyes and adsorbents. The large number of available active sites on adsorbents in the initial stage enables fast dye adsorption, and then the dye adsorption rate on the remaining surface slows down due to the repulsive forces and blocking by the adsorbed dye ions, as the competitive dye adsorption nears equilibrium (Brito et al., 2018). The adsorption of RDY145, RDR195, and RDB222 on MCH was 586.0, 498.0, and 416.7 mg/L, respectively. The dye removal percentage of RDY145 (83.7%) was the highest, followed by RDR195 (71.1%) and RDB222 (59.6%). While CTAB introduced positive charge on ACH surfaces and increased adsorption affinity of MCH for negative dyes, the observed differences in dye removal might be due to dye molecule sizes. Among the three dyes, RDY145 shows the highest adsorption capacity because it is the smallest molecule. The molecular weights of the dyes are shown in Table 1. It should be noted that small-sized molecules could not only adsorb on the adsorbent surface but also possibly penetrated into pores by diffusion and this should increase the adsorption capacity (Vijayaraghavan et al., 2009; Ahmad et al, 2014). In contrast, RDB222 is the largest molecule and its size might complicate the diffusion into the adsorbent pores. The adsorption might occur mainly on the external surfaces of MCH leading to the lowest adsorption efficiency (Ip et al., 2010; Krivova et al., 2013; Ahmad et al., 2014; de Franco et al., 2017).

Additionally, it should be noted that though MCH has a lower surface area than that of AC (data shown in Table 2), the higher RDY145 adsorption capacity using MCH was attributed to the wider average pore diameter of MCH compared to AC. These results are also consistent with the data illustrated in Figure 3 and supported by a study reporting that pore size of adsorbent plays an

important role on adsorbate molecular size and influences its adsorption behavior. Typically, adsorbate molecules could be adsorbed in pores with diameters 1.3-1.8 times their molecular diameter (Ip et al., 2010; Krivova et al., 2013; Ahmad et al., 2014; de Franco et al., 2017). Thus, as shown in Figure 6 (the molecular structure of RDY145 was illustrated by ACD/ChemSketch), a suitable pore size for uptake of RDY145 should be in the range 16.25-22.50 Å. It is seen that the average pore size of AC was below that of MCH, which might slow down the dye adsorption rate.

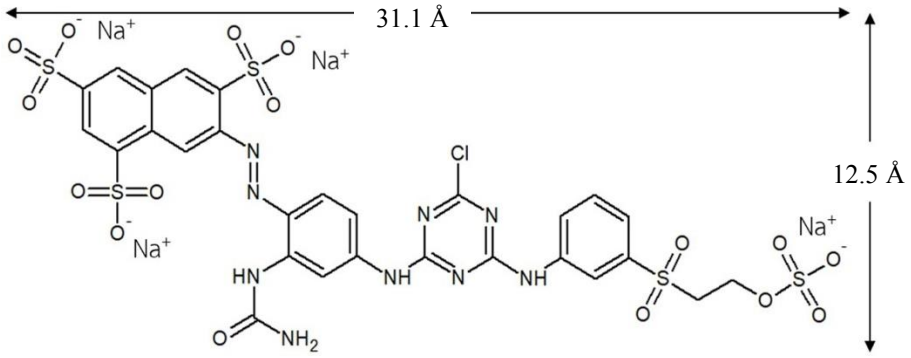

Figure 6. Molecular structure of RDY145

Moreover, AC surface is more hydrophobic than the positively charged MCH surface (Puasa et al., 2018). This non-polar attraction force is weaker than the electrostatic interaction that dominated RDY145 adsorption by MCH, and apparently is not sufficient to enhance the capacity of AC to adsorb the anionic RDY145 (Mi et al., 2016). Therefore, the large pore size of MCH facilitated the diffusion of RDY145 in MCH pores and its adsorption on MCH surfaces, and its positively charged CTAB modified surface provided strong attraction of anionic RDY145 dye molecules, leading to high dye removal efficiency.

Subsequently, the data were fitted with the aforementioned adsorption kinetics models. The kinetic parameters are given in Table 3.

Table 3. Parameters of fitted pseudo-first order and pseudo-second order models for adsorption of reactive dyes by MCH or by AC

Sample	Pseudo-first order			Pseudo-second order		
	k_1 (1/min)	q_e (mg/g)	R^2	k_2 (g/mg-min)	q_e (mg/g)	R^2
MCH-RDY145	0.0184	48.0	0.980	0.00040	68.5	0.997
MCH-RDR195	0.0135	36.5	0.959	0.00071	54.6	0.994
MCH-RDB222	0.0159	34.4	0.939	0.00073	46.5	0.990
AC-RDY145	0.4880	4.8	0.939	0.23700	6.2	0.965

The coefficient of determination (R^2) indicates that the pseudo-second order equation was suitable for fitting the adsorption of all the reactive dyes on MCH and AC. The equilibrium adsorption capacity (q_e) had the rank order RDY145 > RDR195 > RDB222 for reactive dye removal using MCH, and the q_e of MCH-RDY145 was significantly higher than that of AC-RDY145. The results were consistent with the data shown in Figure 5. This suggests that all the dyes were chemically adsorbed irreversibly on the MCH or AC surface and the adsorption rate is controlled by this step (Ibrahim et al., 2010; Ghazi Mokri et al., 2015; Mook et al., 2016). This agrees well with many prior studies (Sun et al., 2013; Ghazi Mokri et al., 2015; Thitame and Shukla, 2016). In addition, the value of k_2 also reflected the dye removal efficiency. A lower value of k_2 indicates higher dye removal. It should be noted that the sort order of k_2 agrees well with the order of q_e, and supports the concept that a small-sized dye could be highly adsorbed with good removal efficiency.

3.5 Equilibrium adsorption of reactive dyes

MCH was used to remove the reactive dyes (RDY145, RDR195, or RDB222) from synthetic wastewater, in experiments labeled as MCH-

RDY145, MCH-RDR195, or MCH-RDB222 shown in Figure 7. The dye adsorption performance of MCH and AC is compared using RDY145 (cases MCH-RDY145 and AC-RDY145) in Figure 7. The adsorbent quantity was controlled at 1 g. The initial dye concentration was varied from 50 to 700 mg/L. The experiment was conducted at pH 7 and 30 °C. The samples were shaken at 170 rpm for 3 h in order to achieve equilibrium. The equilibrium adsorbed reactive dye quantity (q_e) and residual dye concentration are shown in Figure 7. Then, the isotherm data were fitted with the Langmuir and Freundlich isotherms models, and the model parameters are shown in Table 4.

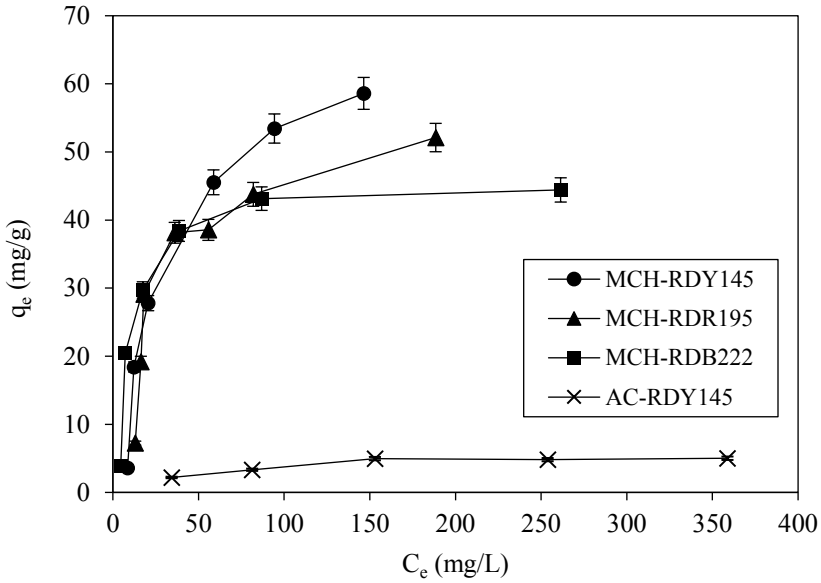

Figure 7. The equilibrium reactive dye adsorption by MCH-RDY145, MCH-RDR195, MCH-RDB222, and AC-RDY145. Operating conditions: 50-700 mg/L of C_0, 30 °C, pH 7, and 170 rpm shaking speed for 3 h.

Table 4. Identified parameters in Langmuir and Freundlich isotherm models for reactive dyes adsorbed by MCH and for RDY145 adsorbed by AC

Dye	Langmuir				Freundlich		
	q_{max} (mg/g)	k_L (L/mg)	R_L	R^2	k_F (mg/g (L/mg)$^{1/n}$)	n	R^2
MCH-RDY145	73.0	0.029	0.0476	1.000	6.30	2.15	0.968
MCH-RDR195	58.8	0.039	0.0354	0.992	9.58	2.94	0.813
MCH-RDB222	46.1	0.104	0.0136	0.999	15.32	4.69	0.855
AC-RDY145	6.4	0.014	0.0930	0.967	0.83	3.22	0.882

The R^2 values of model fits indicate that the Langmuir isotherm was suitable for all the reactive dyes on MCH or RDY145 on AC. According to the Langmuir theory, all reactive dyes were adsorbed on adsorbent surfaces as monolayer. The adsorbent surface was possibly homogenous (Ibrahim et al., 2010; Ghazi Mokri et al., 2015; Mi et al., 2016). The Langmuir parameter q_{max} has the rank order MCH-RDY145 > MCH-RDR195 > MCH-RDB222 > AC-RDY145. These results show similar trends as the experimental data and adsorption kinetics (Figure 5 and Table 3, respectively). Additionally, k_L reveals the interaction forces between adsorbed dye molecules and the surface sites. A higher k_L indicates greater strength of the adsorption forces (Markandeya et al., 2017). The order of k_L values is reversed from the order of q_{max}. For homologous adsorbent, the results confirm that RDB222 has the largest molecules and the least adsorption capacity on MCH (lowest q_{max}), while it had the strongest Van der Waals attraction forces (highest k_L) on MCH. Moreover, the q_{max} of AC-RDY145 was significantly lower than that of MCH-RDY145. Their difference in k_L values indicates that the attraction forces between RDY145 and MCH are much stronger than those with AC, which is consistent with the

aforementioned results (Markandeya et al., 2017). Besides, the values of R_L for all dyes were in the range from zero to one, indicating that adsorption under the experimental conditions were favorable.

Furthermore, many studies have tested various adsorbents obtained from agricultural waste biomass for removing anionic dyes from wastewater, reporting the Langmuir maximum adsorptions q_{max} listed in Table 5. It should be noted that the maximum adsorption capacity was 146.20 mg/g of light green dye on using cationic surfactant (Hexadecylpyridinium bromide, CPB) modified peanut husk (Zhao et al., 2017), while the adsorption capacity was 23.61 mg/g of reactive black 5 using activated carbon from palm shell (Mook et al., 2016). MCH had adsorption capacities in the range 46.10-73.00 mg/g for all three reactive dyes tested. This comparison shows MCH to be an effective adsorbent for reactive dye removal from water.

Table 5. Langmuir isotherm fit based capacities reported by prior studies on adsorption of anionic dye by an adsorbent based on agricultural solid waste

Adsorbent	Dye	q_{max} (mg/g)	Reference
Activated carbon (Palm shell)	Reactive black 5	23.61	Mook et al. (2016)
Activated carbon (*Enteromorpha prolifera*)	Reactive red 23	59.88	Sun et al. (2013)
Activated carbon (*Enteromorpha prolifera*)	Reactive blue171	71.94	Sun et al. (2013)
Activated carbon (*Enteromorpha prolifera*)	Reactive blue 4	131.93	Sun et al. (2013)
CTAB modified Biochar (Cornstalk)	Orange II	26.90	Mi et al. (2016)
CTAB modified wheat straw	Congo red	71.20	Zhang et al. (2014)
CPB modified wheat straw	Light green	70.01	Su et al. (2013)
CPB modified peanut husk	Light green	146.20	Zhao et al. (2017)
MCH	RDY145	73.00	This work
MCH	RDR195	58.80	This work
MCH	RDB222	46.10	This work

4. CONCLUSION

The study demonstrated that the MCH derived from coffee husk was effectively used as an adsorbent to remove reactive dyes (RDY145, RDR195, and RDB222) from synthetic wastewater. The results suggest that wider pores and smaller dye molecules could contribute to adsorption capacity. The mesoporous surface of MCH could enhance the reactive dye-MCH accessibility. Surface modification with CTAB could increase reactive dye removal efficiency by MCH by up to 80%. The dye adsorption kinetics was found to follow the pseudo second-order model. Additionally, the Langmuir isotherm described the dye adsorption equilibrium well. The pH did not significantly affect dye removal performance by MCH. Moreover, MCH provided better dye removal performance than AC. Thus, this work suggests that MCH is a promising adsorbent for reactive dye removal from water, and is comparable to AC and other adsorbents derived from agricultural waste.

ACKNOWLEDGEMENTS

We would like to acknowledge the Thamsing Coffee Group Community Enterprise for supplying coffee husk material, and all the commercial reactive dyes (RDY145, RDR195, and RDB222) were provided by KPT Corporation (Thailand) Co., Ltd. We are grateful for the financial support from the Faculty of Engineering's Graduate Study Scholarship, the Graduate School of Prince of Songkla University (PSU), and for facilities support from the Department of Chemical Engineering, Faculty of Engineering, PSU. Additionally, we would like to thank the PSU research and development office and Assoc. Prof. Seppo Karrila for reviewing the English of this article.

REFERENCES

Ahmad M, Rajapaksha AU, Lim JE, Zhang M, Bolan N, Mohan D, Vithanage M, Lee SS, Ok YS. Biochar as a sorbent for contaminant management in soil and water: a review. Chemosphere 2014;99:19-33.

Amin NK. Removal of reactive dye from aqueous solutions by adsorption onto activated carbons prepared from sugarcane bagasse pith. Desalination 2008;223(1-3):152-61.

Brito MJP, Veloso CM, Santos LS, Bonomo RCF, Fontan R da CI. Adsorption of the textile dye Dianix® royal blue CC onto carbons obtained from yellow mombin fruit stones and activated with KOH and H_3PO_4: kinetics, adsorption equilibrium and thermodynamic studies. Powder Technology 2018;339:334-43.

Department of Industrial Works, Ministry of Industry. Wastewater Management Guidance Manual from Textile Factories. Bangkok, Thailand: Department of Industrial Works, Ministry of Industry; 2013.

de Franco MAE, de Carvalho CB, Bonetto MM, Soares RD, Féris LA. Removal of amoxicillin from water by adsorption onto activated carbon in batch process and fixed bed column: kinetics, isotherms, experimental design and breakthrough curves modelling. Journal of Cleaner Production 2017;161:947-56.

GEO-Informatics Research Center for Natural Resource and Environment, Southern Regional Center of Geo-Informatics and Space Technology. Area of Tham Sing sub-district in Mueang Chumphon District, Chumphon Province, Thailand. Songkhla, Thailand: Prince of Songkla University; 2019.

Ghazi Mokri HS, Modirshahla N, Behnajady MA, Vahid B. Adsorption of C.I. acid red 97 dye from aqueous solution onto walnut shell: kinetics, thermodynamics parameters, isotherms. International Journal of Environmental Science and Technology 2015;12(4): 1401-8.

Guidechem. Reactive Red 195 [Internet]. 2017 [cited 2019 Feb 26]. Available from: https://www.guidechem.com/reference/dic-276579.html#Properties.

Ibrahim S, Fatimah I, Ang HM, Wang S. Adsorption of anionic dyes in aqueous solution using chemically modified barley straw. Water Science and Technology 2010;62(5):1177-82.

Ip AWM, Barford JP, McKay G. A comparative study on the kinetics and mechanisms of removal of reactive black 5 by adsorption onto activated carbons and bone char. Chemical Engineering Journal 2010;157(2-3):434-42.

Ip AWM, Barford JP, McKay G. Reactive black dye adsorption/desorption onto different adsorbents: effect of salt, surface chemistry, pore size and surface area. Journal of Colloid and Interface Science 2009; 337(1):32-8.

Krivova MG, Grinshpan DD, Hedin N. Adsorption of C_nTABr surfactants on activated carbons. Colloids and Surfaces A: Physicochemical and Engineering Aspects 2013;436:62-70.

Kula I, Uğurlu M, Karaoğlu H, Çelik A. Adsorption of Cd(II) ions from aqueous solutions using activated carbon prepared from olive stone by $ZnCl_2$ activation. Bioresource Technology 2008;99(3):492-501.

Lin S-Y, Chen W-f, Cheng M-T, Li Q. Investigation of factors that affect cationic surfactant loading on activated carbon and perchlorate adsorption. Colloids and Surfaces A: Physicochemical and Engineering Aspects 2013;434:236-42.

Maleangpoothong J, Photha P, Siriwongyotha C, Paksa W, Rommanee W, Taweesuk D, Srichoo C. Thailand experiences from the grassroots: value chain finance best practices, initiatives, strategies and trends in agriculture. Bangkok, Thailand: Asia-Pacific Rural and Agricultural Credit Association; 2013.

Markandeya, Shukl SP, Dhiman N. Characterization and adsorption of disperse dyes from wastewater onto cenospheres activated carbon composites. Environmental Earth Sciences 2017;76(20):1-12.

Meng L, Xu X, Bai B, Ma M, Li S, Hu N, Wang H, Suo Y. Surface carboxyl-activated polyester (PET) fibers decorated with glucose carbon microspheres and their enhanced selective adsorption for dyes. Journal of Physics and Chemistry of Solids 2018;123:378-88.

Mi X, Li G, Zhu W, Liu L. Enhanced adsorption of orange II using cationic surfactant modified biochar pyrolyzed from cornstalk. Journal of Chemistry 2016;2016:1-7.

Moazzam A, Jamil N, Nadeem F, Qadir A, Ahsan N, Zameer M. Reactive dye removal by a novel biochar/MgO nanocomposite. Journal of the Chemical Society of Pakistan 2017;39(1):26-34.

Mook WT, Aroua MK, Szlachta M. Palm shell-based activated carbon for removing reactive black 5 dye: equilibrium and kinetics studies. BioResources 2016;11(1):1432-47.

Mozammel HM, Masahiro O, Bhattacharya SC. Activated charcoal from coconut shell using $ZnCl_2$ activation. Biomass and Bioenergy 2002;22(5):397-400.

Nabil GM, El-mallah NM, Mahmoud ME. Enhanced decolorization of reactive black 5 dye by active carbon sorbent-immobilized-cationic surfactant (AC-CS). Journal of Industrial and Engineering Chemistry 2014;20(3):994-1002.

National Center for Biotechnology Information (NCBI). PubChem Compound Database; CID=5974 [Internet]. 2004 [cited 2018 Jul 30]. Available from: https://pubchem.ncbi.nlm.nih.gov/compound/5974.

National Center for Biotechnology Information (NCBI). PubChem Compound Database; CID=157317 [Internet]. 2005 [cited 2018 Jul 20]. Available from: https://pubchem.ncbi.nlm.nih.gov/compound/157317.

National Center for Biotechnology Information (NCBI). PubChem Compound Database; CID=102407104 [Internet]. 2015 [cited 2018 Jul 20]. Available from: https://pubchem.ncbi.nlm.nih.gov/compound/102407104.

Oei BC, Ibrahim S, Wang S, Ang HM. Surfactant modified barley straw for removal of acid and reactive dyes from aqueous solution. Bioresource Technology 2009;100(18):4292-5.

Ogugbue CJ, Sawidis T. Bioremediation and detoxification of synthetic wastewater containing triarylmethane dyes by aeromonas hydrophila isolated from industrial effluent. Biotechnology Research International 2011;2011:1-11.

Puasa SW, Ismail KN, Khairi NAIA. Direct surfactant-impregnated activated carbon for adsorption of reactive blue 4. International Journal of Engineering and Technology 2018;7(4):5-8.

Rehman HA, Razzaq R. Benefits of biochar on the agriculture and environment: a review. Journal of Environmental Analytical Chemistry 2017;4(3):1-3.

Su Y, Zhao B, Xiao W, Han R. Adsorption behavior of light green anionic dye using cationic surfactant-modified wheat straw in batch and column mode. Environmental Science and Pollution Research 2013;20(8):5558-68.

Sun D, Zhang Z, Wang M, Wu Y. Adsorption of reactive dyes on activated carbon developed from *Enteromorpha prolifera*. American Journal of Analytical Chemistry 2013;4(7A):17-26.

Thitame PV, Shukla SR. Adsorptive removal of reactive dyes from aqueous solution using activated carbon synthesized from waste biomass materials. International Journal of Environmental Science and Technology 2016;13(2):561-70.

Vijayaraghavan K, Won SW, Yun Y-S. Treatment of complex Remazol dye effluent using sawdust- and coal-based activated carbons. Journal of Hazardous Materials 2009; 167(1-3):790-6.

Wang X, Jiang C, Hou B, Wang Y, Hao C, Wu J. Carbon composite lignin-based adsorbents for the adsorption of dyes. Chemosphere 2018;206:587-96.

Zhang R, Zhang J, Zhang X, Dou C, Han R. Adsorption of Congo red from aqueous solutions using cationic surfactant modified wheat straw in batch mode: kinetic and equilibrium study. Journal of the Taiwan Institute of Chemical Engineers 2014;45(5):2578-83.

Zhao B, Xiao W, Shang Y, Zhu H, Han R. Adsorption of light green anionic dye using cationic surfactant-modified peanut husk in batch mode. Arabian Journal of Chemistry 2017;10(Supplement 2):S3595-602.